Supporting Information

Ghosh et al. 10.1073/pnas.1120755109

SI Methods

Antibodies and Reagents. Antibodies to Tie-2 (clone Ab33), phospho-Tie-2-Y992 (#09407 for immunostaining), GAPDH, C-terminal MEK1/2, and N-terminal MEK1/2 were purchased from Upstate/Millipore. Tie-2 (C-20), angiopoietin-2 (Angpt-2; F-18), and actin antibodies were purchased from Santa Cruz. Antibodies to phospho-MEK1/2, ERK1/2, phospho-ERK1/2, Akt and phospho-Akt (Ser-473), caspase and cleaved caspase-3, and phospho-Tie-2-Y992 (#4221 for Western blotting) were from Cell Signaling. Anti–VE-cadherin and anti–CD-31 were purchased from BD Bioscience. Fluorophore- or HRP-conjugated secondary antibodies were purchased from Invitrogen, as were phalloidin and DAPI. Recombinant human angiopoietin-1 (Angpt-1) and anti–Angpt-2 antibody (monoclonal) were purchased from R&D Systems. Recombinant protective antigen (PA), lethal factor (LF), and E687C LF were purchased from List Biological Laboratories and were used in a 1:1 ratio [e.g., 50 μg of lethal toxin (LT) equals 50 μg PA plus 50 μg LF] in all experiments. Adenovirus expressing Angpt-1 (Ad-Angpt-1) was obtained from S. Wiegand (Regeneron Pharmaceuticals, Tarrytown, NY), and control adenovirus (Ad-CMV-GFP) was from Vector Biolabs. Lentiviruses encoding uncleavable MEK1 and MEK2 in combination with EGFP (lenti-MEK1/2) or EGFP alone (lenti-GFP) were described previously (1). Angpt-1 was measured by commercial ELISA (R&D Systems). Other chemicals were purchased from Sigma.

Quantitative PCR. Total RNA was extracted using TRIzol (Invitrogen) followed by clean-up using the RNeasy Mini Kit with on-column DNase digestion (QIAGEN) according to the manufacturer's instructions. Total RNA then was reverse transcribed to cDNA, and PCR reactions were performed using either TaqMan (QIAGEN) or SYBR Green on the ABI 7500 Fast Real-Time PCR System (Applied Biosystems) at the multigene transcriptional profiling core at Beth Israel Deaconess Medical Center (http://cvbr.hms.harvard.edu/CORErealtimePCR.html; primers are available upon request). Expression levels relative to the housekeeping control (18S rRNA) were determined using the comparative threshold method, and results were normalized by their respective experimental controls.

Western Blot Analysis. Cells were washed twice with ice-cold PBS and lysed with ice-cold RIPA buffer [50 mM Tris·HCl (pH 7.4), 150 mM NaCl, 1% Nonidet P-40, 0.5% sodium deoxycholate, 0.1% SDS, and 1 mM EDTA] supplemented with protease inhibitors (Roche Diagnostics), 1 mM $NaVO_4$, and 1 mM NaF. Lysates were sonicated and centrifuged at 10,000 rpm for 10 min at 4 °C, and supernatants were collected. Protein concentrations were determined by Bradford protein assay with BSA as a standard (Bio-Rad). A mixture of lysate, NuPAGE reducing agent, and NuPAGE sample buffer was heated at 70 °C for 10 min, electrophoresed in NuPAGE 4–12% Novex Bis-Tris gels (all from Invitrogen), transferred to nitrocellulose membrane, and immunoblotted with specific primary antibodies. Binding of primary antibodies was detected using HRP-conjugated secondary antibodies (Amersham Pharmacia Biotech) and SuperSignal West-Dura (Pierce) reagents as chemiluminescence substrates.

Immunoprecipitation. For serum immunoprecipitation of Angpt-2, 150 μL of serum from individual mice was incubated with polyclonal anti–Angpt-2 antibody for 12 h at 4 °C. Magnetic Dynabeads conjugated with protein G (Invitrogen) were added for 45 min at 4 °C to precipitate the antigen–antibody complex. After the beads were washed, proteins were eluted by heating in lithium dodecyl sulfate sample and elution buffer and were detected by Western blot analysis with monoclonal anti–Angpt-2 antibody.

Immunocytochemistry. Human microvascular endothelial cells (HMVECs) were grown to confluence on glass coverslips coated with Attachment factor (Mediatech). The cells were fixed for 10 min in 3% paraformaldehyde and were permeabilized for 5 min in 0.2% Triton X-100 in PBS. Cells then were blocked for 30 min with 1% BSA in PBS, incubated for 2 h with primary antibody, washed serially in PBS, then secondary antibody and phalloidin. The coverslips were mounted using ProLong Gold antifade reagent with DAPI. All images were taken by a Zeiss LSM510 META confocal system at 63× magnification. Of note, all images presented were obtained with the same laser power, gain, and offset conditions.

Immunohistochemistry. Air-dried periodate-lysine-paraformaldehyde–fixed cryosections from lungs were blocked for 60 min in 10% donkey serum and then were incubated with primary antibodies overnight at 4° C, followed by fluorescence-conjugated affinity-purified secondary antibody labeling (60 min; 1:500) (Jackson), and were mounted with ProLong Gold/DAPI. All images were taken by a Zeiss LSM510 META confocal system at 63× magnification. Of note, all images were obtained with the same laser power, gain, and offset conditions.

Histopathology. Mouse lungs were excised 72 h after LT injection and were insufflated gently over 2 min to total lung capacity with 2 mL formalin delivered through a secured syringe placed in the trachea. The trachea then was ligated distal to the insufflation site, and the heart–lung block was removed carefully and placed into formalin *en caul*. Liver and kidney also were harvested, and the organs were fixed overnight in formalin, embedded in paraffin, sectioned, and stained with H&E. Bronchovascular bundles were identified in transverse cross-sections of the lower third of heart–lung blocks.

Evans Blue Permeability Assay. Animals were anesthetized with inhaled isoflurane 72 h after i.v. injection of LT, and 50 μL Evans blue (2% wt/vol) was injected into the retroorbital sinus. Mice were killed 10 min after Evans blue injection and were perfused with 10 mL of PBS and 2 mM EDTA for 5 min through a cannula placed in the right ventricle. Then organs were harvested and homogenized in formamide for extraction and measurement of Evans Blue as previously described (2). The following formula was used to correct the optical densities for contamination with heme pigments:

$$\mathrm{E620(corrected)} = \mathrm{E620(raw)} - (1.426 \times \mathrm{E740(raw)} + 0.030)$$

Transwell Permeability Assay. Confluent HMVEC monolayers were grown on collagen-1–coated Costar Transwell membranes (polyester 0.4-μm filter) (Corning), and permeability was determined by measurement of fluorometric signal in the luminal and abluminal chambers at the indicated time points after luminal addition of 1 mg/mL FITC-labeled human serum albumin (Sigma) as described previously. Relative fluorescence units were used in the following equation to determine the permeability coefficient of albumin (P_a):

$$P_a/\mathrm{hr} = [A]/[L] \times V/tA$$

where $[A]$ is abluminal concentration; $[L]$ is luminal concentration; V is volume of abluminal chamber; t is time in hours; and A is the area of membrane in square centimeters.

Lentiviral Transduction. Lentiviral particle generation has been described elsewhere (1). HMVECs of passage 3 were used for lentiviral transduction. Cells cotransduced with noncleavable MEK1 and MEK2 mutants together were sorted for medium EGFP-expressing cells by flow cytometry (FACS Vantage DiVa; BD Biosciences). MEK1/2 and EGFP expression in HMVECs was verified by Western blotting and immunofluorescence, respectively.

1. Lehmann M, Noack D, Wood M, Perego M, Knaus UG (2009) Lung epithelial injury by B. anthracis lethal toxin is caused by MKK-dependent loss of cytoskeletal integrity. *PLoS ONE* 4:e4755.

2. Parikh SM, et al. (2006) Excess circulating angiopoietin-2 may contribute to pulmonary vascular leak in sepsis in humans. *PLoS Med* 3:e46.

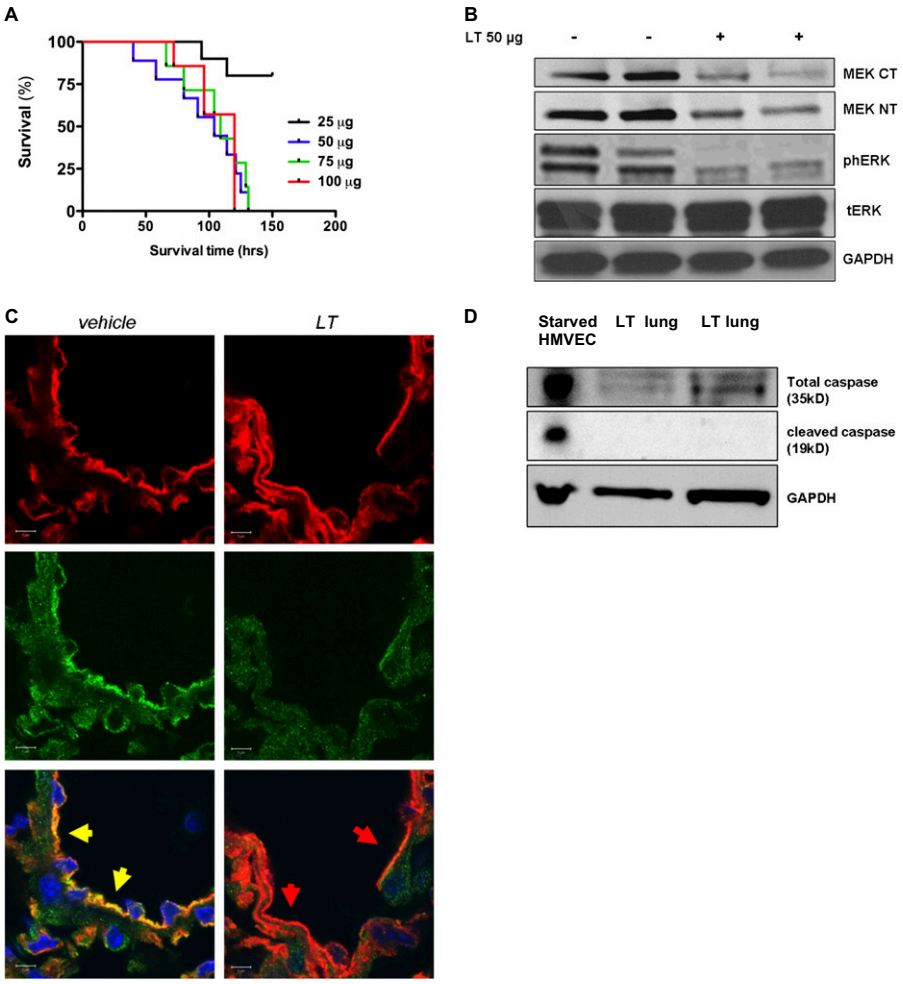

Fig. S1. General features of the i.v. LT model in C57BL6J mice. (*A*) Survival curves following different i.v. doses of LT in 8-wk-old male C57BL6J mice (25 μg, n = 9; 50 μg, n = 9; 75 μg, n = 6; 100 μg, n = 7). The lowest dose that resulted in a mortality of 100% (i.e., 50 μg) was used for subsequent experiments. (*B*) Representative immunoblots of the MEK1/2–ERK1/2 pathway in lung homogenates from individual mice 72 h after i.v administration of vehicle or 50 μg LT. MEK CT, C-terminal anti-MEK1/2 antibody; MEK NT, N-terminal anti-MEK1/2 antibody; phERK, phospho-ERK1/2; tERK, total ERK1/2. Data shown are representative of three to five mice per group. (*C*) Fluorescent immunohistochemistry for VE-cadherin (green) and the endothelial marker CD31 (red) of larger blood vessels from murine lungs 72 h after i.v. administration of vehicle or 50 μg LT. Arrows point to endothelium. Images shown are representative of five animals per group. (Scale bar: 5 μm.) (*D*) Immunoblot for total and cleaved caspase-3 from positive control (*Left*, serum starvation induced apoptosis of HMVECs) and representative homogenates of lung collected 72 h after i.v. administration of 50 μg LT.

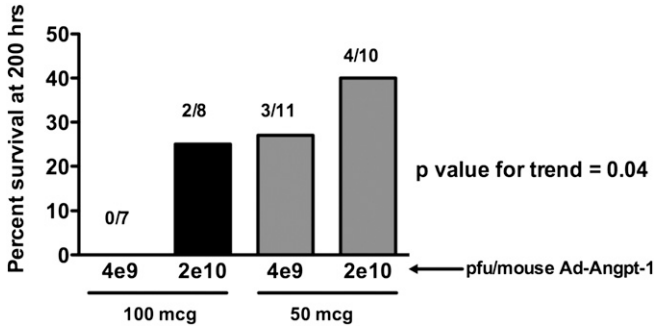

Fig. S2. Dose-ranging pilot studies for Ad-Angpt-1 (AdAngpt-1) and LT. Percent survival 200 h after i.v administration of 50 or 100 μg LT in 8- to 10-wk-old C57BL6J male mice pretreated with one of two doses of Ad-Angpt-1 (4×10^9 or 2×10^{10} particle-forming units) via tail vein injection 48 h before LT injection. Fractions above each bar indicate the number of surviving animals from the total number of animals administered LT. *P* was determined by ANOVA.

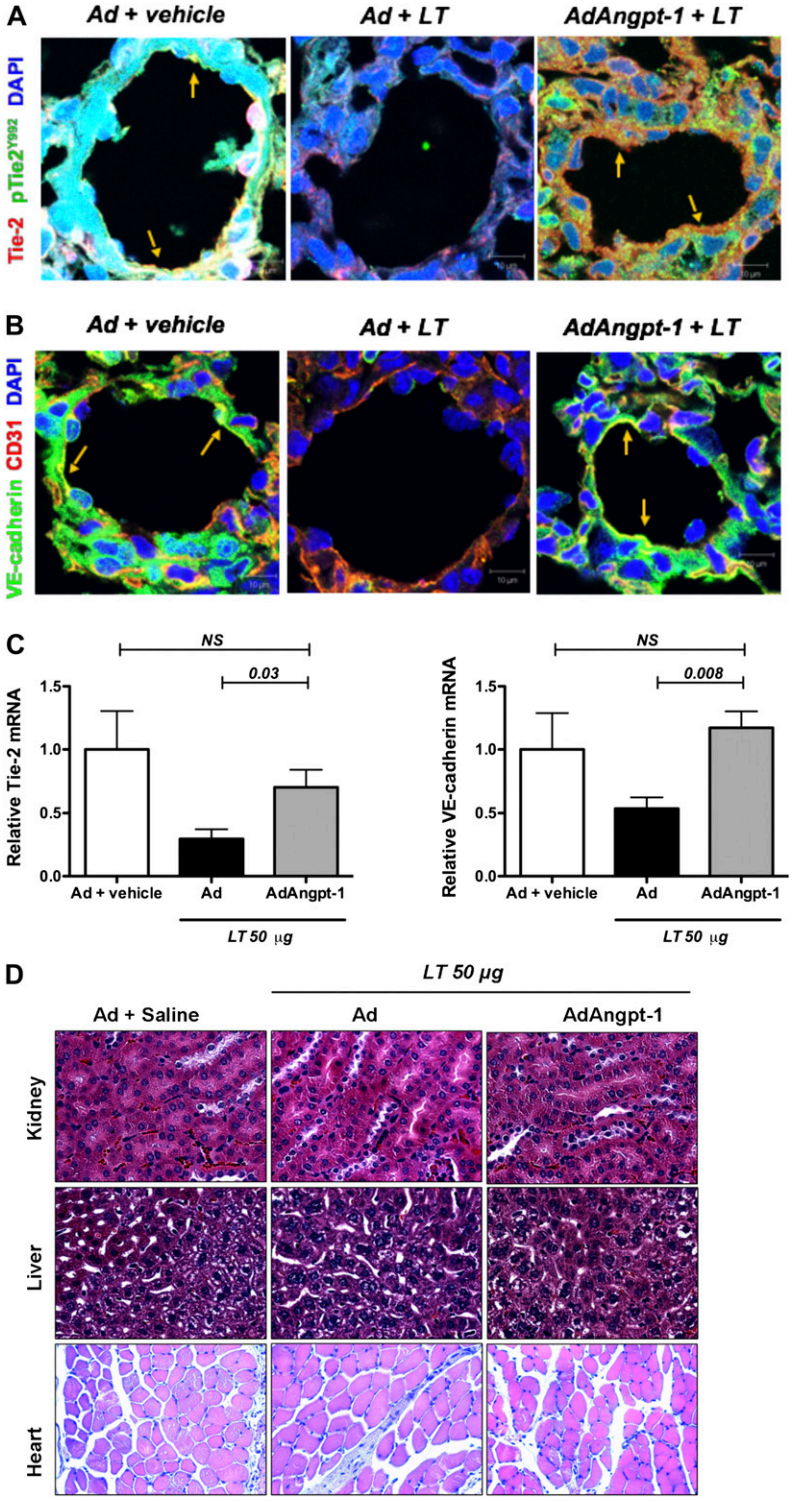

Fig. S3. Tie-2 levels and phosphorylation are depressed following LT challenge. (*A*) Fluorescent immunohistochemistry for Tie-2 (red) and pTie-2 (Y992) (green) from lungs 72 h after vehicle or LT challenge in mice pretreated with control adenovirus (Ad) or Ad-Angpt-1 (AdAngpt-1). Arrows indicate endothelium. Images shown are representative of five animals per group. Phosphorylation of Tie-2 results in colocalization appearing as yellow in the merged image. (Scale bar: 10 μm.) (*B*) Fluorescent immunochemistry from above conditions for VE-cadherin (green) and CD31 (red). Arrows indicate endothelium. Images shown are representative of five animals per group. (Scale bar: 10 μm.) (*C*) Real-time PCR of lung homogenates for Tie-2 and VE-cadherin mRNA 72 h after administration of vehicle or LT with control adenovirus (Ad) or Ad-Angpt-1 (AdAngpt-1) pretreatment. $n = 3–5$ mice per condition. $P < 0.05$ by ANOVA for Tie-2 and VE-cadherin and pairwise P values as indicated. (*D*) Examples of renal, hepatic, and cardiac histology 72 h after administration of 50 μg LT following pretreatment with control adenovirus (Ad) or A-Angpt-1 (AdAngpt-1).

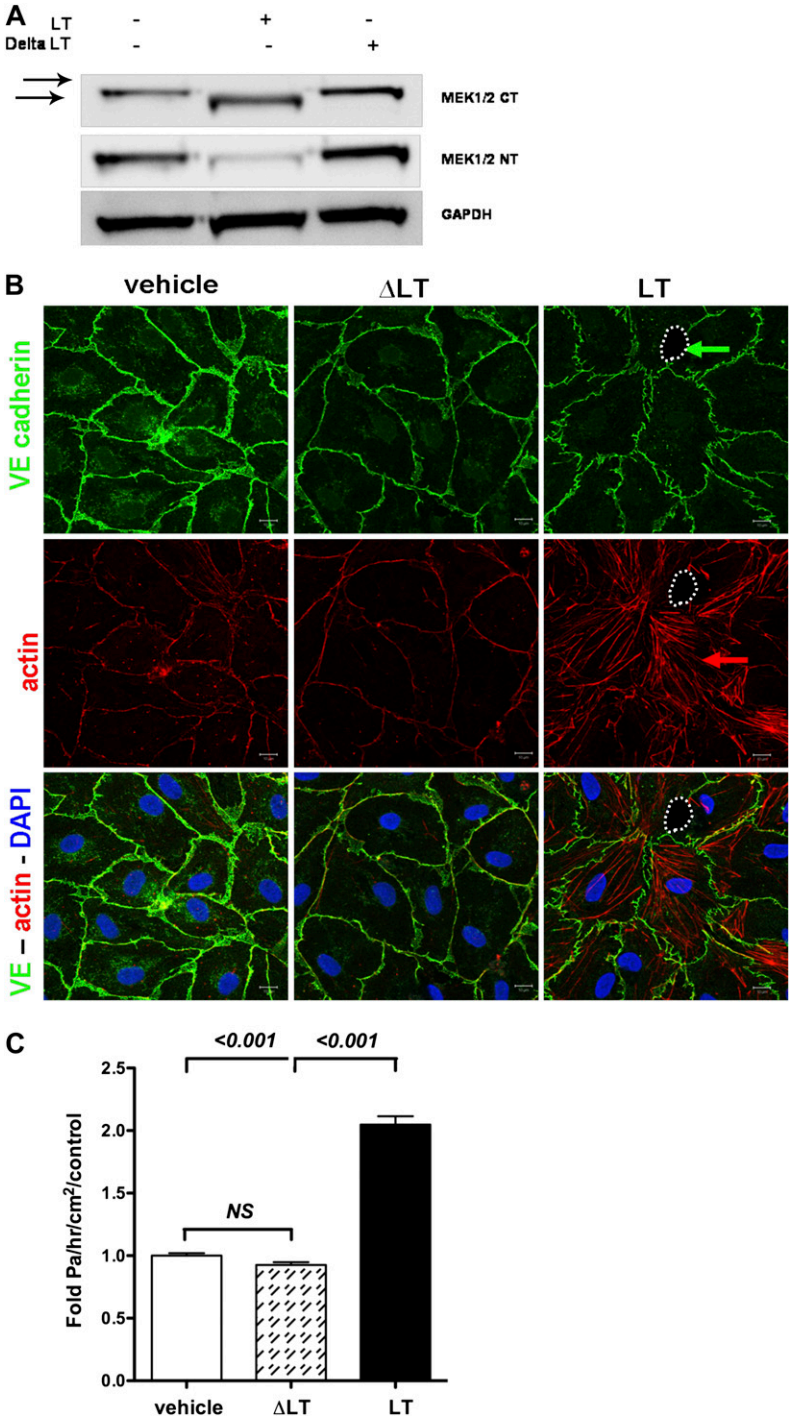

Fig. S4. Enzymatic activity of LT is necessary for molecular, structural, and functional effects of LT on microvascular endothelial cells. (*A*) Lysates of HMVECs treated for 7 h with 1 μg/mL of LT or 1 μg/mL of catalytically inactive (E687C) LT (Δ*LT*), blotted with C-terminal anti-MEK1/2 [*Top*, demonstrating downward shift of cleaved protein (arrows)], N-terminal anti-MEK1/2 (*Middle*, demonstrating loss of N-terminal epitope), and anti-GAPDH (*Bottom*). (*B*) Immunofluorescence on HMVECs subjected to above treatments for 24 h. Green arrow and white dotted circles indicate a paracellular gap; the red arrow indicates actin stress fibers. (*C*) Transwell permeability assay performed on HMVECs subjected to above treatments. $P < 0.0001$ by ANOVA with post hoc pairwise *P* values as indicated. NS, not significant.

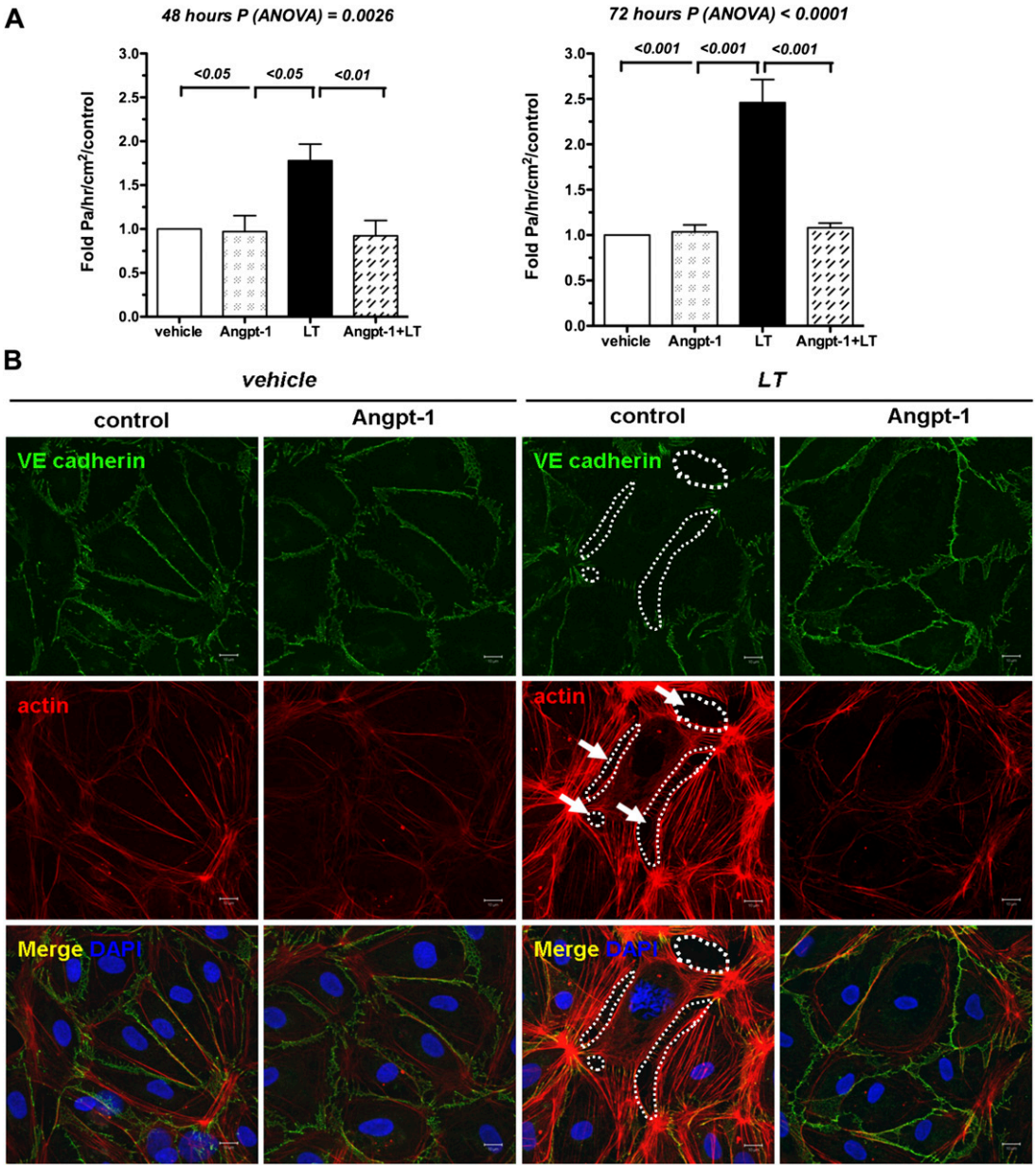

Fig. S5. Angpt-1 abrogates LT-induced endothelial barrier dysfunction. (*A*) Transwell permeability assay performed on confluent HMVECs treated with vehicle, Angpt-1 (500 ng/mL), and/or LT (100 ng/mL) for 48 or 72 h (n = 3–6 independent experiments per condition, normalized by average response of vehicle-treated cells). *P* by ANOVA and post hoc pairwise *P* values as indicated. (*B*) Fluorescent immunocytochemistry performed on HMVECs treated with vehicle, Angpt-1 (500 ng/mL), and/or LT (100 ng/mL**)** for 24 h showing interendothelial junctions (green, anti–VE-cadherin), F-actin (red, phalloidin), and nuclei (blue, DAPI). White arrows and dotted circles indicate interendothelial gaps. Images are representative of three experiments per condition. (Scale bar: 10 μm.)

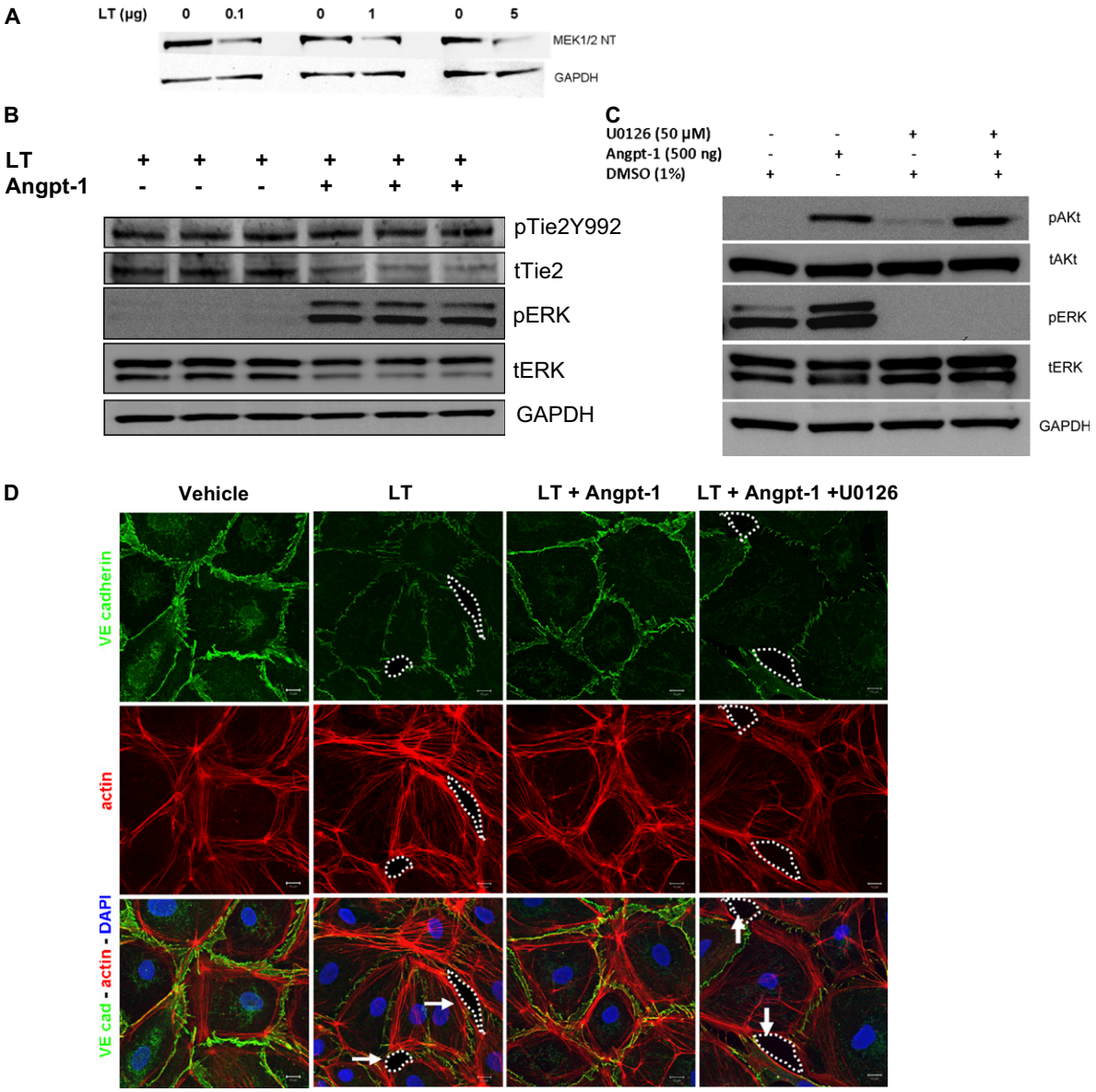

Fig. S6. MEK-dependent ERK1/2 activation in Angpt-1–mediated barrier defense against LT. (*A*) A small fraction of endogenous MEK1/2, as detected by anti–N-terminal MEK1/2 antibody, persists in HMVECs at 7 h despite high dose of LT (numbers indicate micrograms per milliliter of LT). (*B*) Representative immunoblots of HMVEC lysates after treatment with LT (1 μg) for 48 h followed by Angpt-1 (500 ng) for 10 min. (*C*) Immunoblots from HMVECs treated with U0126 (50 μM in 1% DMSO) for 60 min followed by Angpt-1 (500 ng/mL) for 10 min with anti–phospho-Akt (pAkt), anti-Akt (tAkt), anti–phospho-ERK1/2 (pERK), anti-ERK1/2 (tERK), and anti-GAPDH. (*D*) Fluorescent immunocytochemistry after treatment with vehicle, LT (100 ng/mL), Angpt-1 (500 ng/mL), and U0126 (50 μM). White arrows and dotted circles indicate interendothelial gaps. Images are representative of five experiments per condition. (Scale bar: 10 μm.)

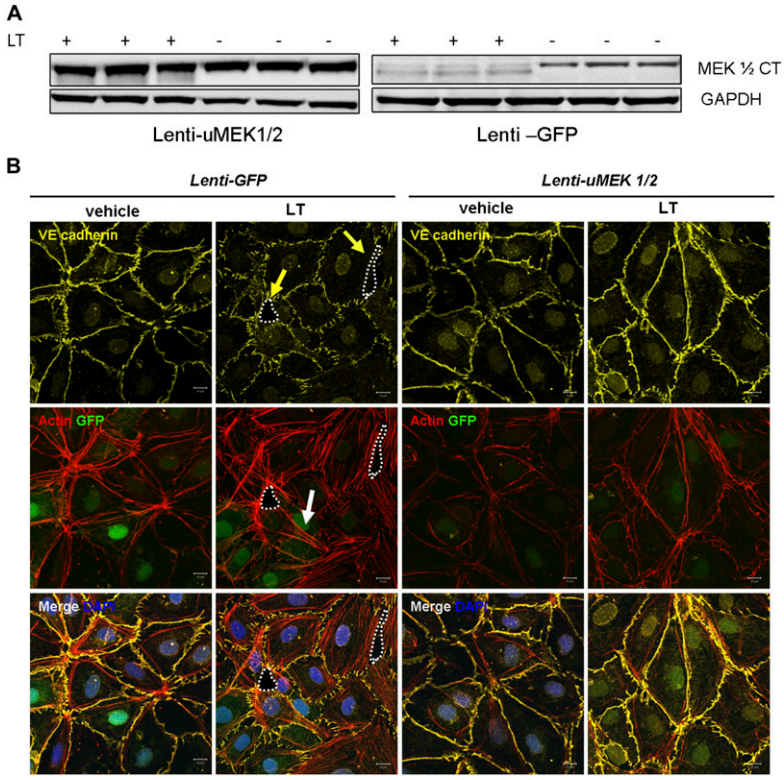

Fig. S7. Uncleavable isoforms of MEK1 and MEK2 prevent LT-induced endothelial barrier disruption. (*A*) Immunoblot of lysates for MEK1/2 from HMVECs transfected with lenti-GFP or lenti-uncleavable MEK1/2 (lenti-uMEK1/2) and then treated with 1 μg/mL LT for 7 h. Membranes were blotted with anti–C-terminal-MEK1/2 (MEK1/2 CT). In cells expressing uMEK1/2, cleavage of the endogenous protein by LT is demonstrated by the lower-molecular-weight band. In lenti-GFP–treated cells, LT application reduces the abundance of MEK1/2, and a doublet band is visible, with the lower band reflecting the cleavage product. (*B*) Fluorescent immunocytochemistry of HMVECs transduced with lenti-GFP or lenti-uncleavable MEK1/2 (lenti-uMEK1/2) after 24 h of treatment with 1 μg/mL LT or vehicle, showing GFP (green), F-actin (red, phalloidin), and interendothelial junctions (yellow, anti–VE-cadherin). Images shown are representative of three experiments per condition. Yellow arrows and white dotted circles indicate interendothelial gaps; the white arrow indicates actin stress fibers.

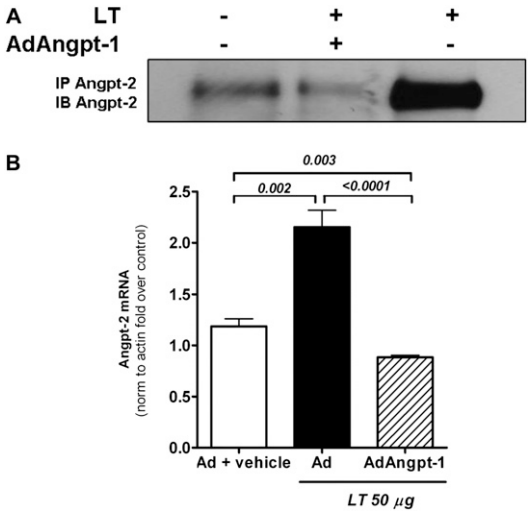

Fig. S8. Induction of Angpt-2 in the mouse anthrax LT model. (*A*) Immunoprecipitation for Angpt-2 (polyclonal rabbit; Santa Cruz) followed by blotting with a mouse monoclonal Angpt-2 Ab (R&D Systems) from 150 μL mouse serum treated with control adenovirus (–) or AdAngpt-1 (+) and either vehicle or 50 μg LT. Each lane represents immunoprecipitation of a single mouse's serum 72 h after LT administration. Results are representative of four mice per condition. (*B*) Bar graphs showing relative abundance of Angpt-2 transcript in lungs obtained 72 h after treatment with LT or vehicle with or without Ad-Angpt-1 (AdAngpt-1) pretreatment. Results analyzed by ANOVA, $P < 0.0001$ with post hoc pairwise P values as indicated. $n = 5$ animals per condition.

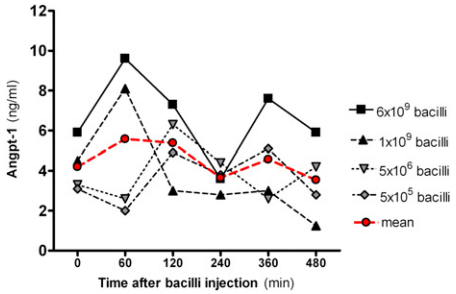

Fig. S9. Angpt-1 trends in baboons over time. Four adult baboons were inoculated i.v. at time 0 with different doses of toxigenic 34F2 Sterne strain anthrax bacilli. Venous blood was collected at serial time points. Angpt-1 levels were measured longitudinally (0, 1, 2, 4, 6, and 8 h) by ELISA.

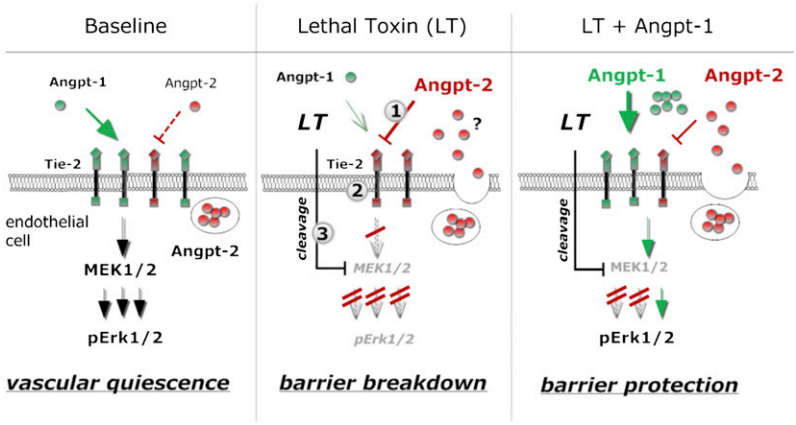

Fig. S10. Intersecting pathways of LT and the Angpt–Tie-2 signaling axis in the endothelium. (*Left*) Under basal conditions, Tie-2 is phosphorylated by local Angpt-1 (indicated by green receptors), promoting vascular quiescence, MEK-dependent ERK1/2 activation, and barrier function, as previously shown (1–3). (*Center*) Exposure to anthrax LT induces (*i*) the up-regulation of Angpt-2 (Fig. S8) and (*ii*) suppression of Tie-2 expression (Fig. 1). Either of these changes alone is sufficient to reduce signaling through the Tie-2 receptor. When these changes are combined, the suppressive effect on Tie-2 activity is dramatic (Figs. 1 and 3 and Fig. S3). Furthermore, (*iii*) LT directly inactivates MEK1/2, the downstream signaling target of Tie-2. These coordinated changes upstream of, including, and downstream of Tie-2 contribute to barrier breakdown (Figs. 1 and 3 and Figs. S3 and S4). (*Right*) Addition of Angpt-1 prevents lethality (Fig. 2), enhances Tie-2 activation (Fig. 3), and prevents resultant vascular leakage (Fig. 3) but requires MEK-dependent signaling to do so (Fig. 4). Expression of uncleavable MEK1/2 isoforms recapitulates the actions of Angpt-1 (Fig. 4). Finally, imbalance in angiopoietins is a prominent and early feature of anthrax bacteremia in primates (Fig. 5).

1. Wong AL, et al. (1997) Tie2 expression and phosphorylation in angiogenic and quiescent adult tissues. *Circ Res* 81:567–574.
2. Thurston G, et al. (2000) Angiopoietin-1 protects the adult vasculature against plasma leakage. *Nat Med* 6:460–463.
3. Harfouche R, et al. (2003) Angiopoietin-1 activates both anti- and proapoptotic mitogen-activated protein kinases. *FASEB J* 17:1523–1525.